Sussex Research Online

The Creation and Detection of Arbitrary Photon Number States Using Cavity QED

Article (Published Version)

Varcoe, Benjamin T H, Brattke, Simon and Walther, Herbert (2004) The Creation and Detection of Arbitrary Photon Number States Using Cavity QED. New Journal of Physics, 6 (1). p. 97. ISSN 1367-2630

This version is available from Sussex Research Online: http://sro.sussex.ac.uk/28494/

This document is made available in accordance with publisher policies and may differ from the published version or from the version of record. If you wish to cite this item you are advised to consult the publisher's version. Please see the URL above for details on accessing the published version.

Copyright and reuse:
Sussex Research Online is a digital repository of the research output of the University.

Copyright and all moral rights to the version of the paper presented here belong to the individual author(s) and/or other copyright owners. To the extent reasonable and practicable, the material made available in SRO has been checked for eligibility before being made available.

Copies of full text items generally can be reproduced, displayed or performed and given to third parties in any format or medium for personal research or study, educational, or not-for-profit purposes without prior permission or charge, provided that the authors, title and full bibliographic details are credited, a hyperlink and/or URL is given for the original metadata page and the content is not changed in any way.

http://sro.sussex.ac.uk

IOPscience iopscience.iop.org

The creation and detection of arbitrary photon number states using cavity QED

This content has been downloaded from IOPscience. Please scroll down to see the full text.

View the table of contents for this issue, or go to the journal homepage for more

Download details:

IP Address: 84.92.41.220
This content was downloaded on 17/06/2014 at 15:13

Please note that terms and conditions apply.

New Journal of Physics
An Institute of Physics and Deutsche Physikalische Gesellschaft Journal

The creation and detection of arbitrary photon number states using cavity QED

Benjamin T H Varcoe[1], **Simon Brattke**[2] **and Herbert Walther**[2,3]

[1] Physics and Astronomy, University of Sussex, Falmer, Brighton BN1 9QH, UK

[2] Max Planck Institute for Quantum Optics, Garching Bei München, D85748, Germany

E-mail: B.Varcoe@sussex.ac.uk or H.Walther@mpq.mpg.de

New Journal of Physics **6** (2004) 97
Received 16 February 2004
Published 29 July 2004
Online at http://www.njp.org/
doi:10.1088/1367-2630/6/1/097

Abstract. Many applications in quantum information or quantum computing require radiation with a fixed number of photons (called Fock or number states) and this special issue demonstrates the real increase in interest in this area. In this paper, we review three recent papers in which we discussed the creation of photon number states in the micromaser and discuss new results. In the first experiment, Fock states were created in steady state via trapping states. Some new results are presented in this section showing a remarkable improvement of our ability to create these states. We then review a second method of dynamic Fock state creation using state reduction of lower state atoms. In this experiment, we also observed the purity of the Fock state that was created via the observation of Rabi oscillations of a probe atom. Finally, we discuss the results of the third experiment that we performed which was an experimental demonstration of a method of creating Fock states on demand.

[3] Author to whom any correspondence should be addressed.

PII: S1367-2630(04)76200-X
© IOP Publishing Ltd and Deutsche Physikalische Gesellschaft

Contents

1. Introduction

The one-atom maser or micromaser represents the most basic system in cavity quantum electrodynamics. In the micromaser highly excited Rydberg atoms interact with a single mode of a superconducting cavity with a high-quality factor that leads to very long photon lifetimes. Thus, in the micromaser, a single atom interacts with a single mode of the radiation field [1]. It thus represents the simple system treated in the Jaynes–Cummings model [2] in the early days of masers and lasers [3]. The steady-state field generated in the cavity has already been the object of detailed studies of the sub-Poissonian statistical distribution of the field [4], the quantum dynamics of the atom-field photon exchange represented in the collapse and revivals of the Rabi nutation [5], atomic interference [6], bistability and quantum jumps of the field [7], and atom–field and atom–atom entanglement [8].

The quantum treatment of the radiation field uses the number of photons in a particular mode to characterize the quantum states whereby in the ideal case the modes are defined by the boundary conditions of a cavity giving a discrete set of eigenfrequencies. The ground state of the quantum field is represented by the vacuum state consisting of field fluctuations with no residual energy. The states with fixed photon number are usually called Fock or number states. They are generally used as the basis for the quantum representation of radiation fields. Number states thus represent the most basic quantum states and are maximally distant from what one would call a classical field. Although number states of vibrational motion are routinely observed in ion traps [9], number states of the radiation field are very fragile and very difficult to produce and maintain. They are perfectly number-squeezed, extreme sub-Poissonian states in which intensity fluctuations vanish completely. In order to generate these states, it is necessary that the mode considered has minimal losses and the thermal field, always present at finite temperatures, can be eliminated since it causes photon number fluctuations.

In this paper, we briefly review three recent experiments in which the creation of photon number states in the micromaser was demonstrated and, in addition, new results as an extension of those experiments will be reported. We observed Fock states via a steady-state feature called trapping states both as a function of interaction time and as a function of the frequency of the cavity [10]–[12]; furthermore by state reduction of lower state atoms [12]–[14] and finally we demonstrated a source of photon Fock states on demand [12, 15, 16].

2. Micromaser theory

In the Jaynes–Cummings Hamiltonian [2], describing the single-atom–single-mode system, there are no dissipative losses, therefore spontaneous emission is reversible and two level atoms undergo Rabi oscillations in the presence of a photon number $|n\rangle$, where $n = 0, 1, 2, \ldots$. Under this influence, the relative populations of the excited and ground states of an atom will oscillate at a frequency $\Omega\sqrt{n+1}$, where Ω is the atom–field coupling constant. Experimentally, we measure the atomic inversion, which is given by $I = P_g - P_e$ where P_g and P_e are the probabilities of finding ground and excited state atoms, respectively. For an n photon Fock state this interaction produces Rabi oscillations which are given by

$$I(t_{\text{int}}) = -\cos(2\Omega\sqrt{n+1}t_{\text{int}}). \tag{1}$$

A more general occurrence is for the field to be an admixture of Fock states, in which case we write

$$I(t_{\text{int}}) = -\sum_n P_n \cos(2\Omega\sqrt{n+1}t_{\text{int}}), \tag{2}$$

where P_n is the probability of finding n photons in the mode, and t_{int} is the interaction time of the atoms with the cavity field. In the one-atom maser the atom–atom spacing can easily be shorter than the lifetime of photons in the mode (up to 0.3 s), thus leading to a buildup of a steady-state field in the cavity. The steady-state field is created via a trade off between the Jaynes–Cummings interaction of single atoms and the cavity field and the (small) dissipation that occurs between atoms. The micromaser has been the subject of a large number of theoretical and experimental papers and is now a textbook subject [2]. The steady-state field is described by the formula

$$P_n = C\left(\frac{n_{\text{th}}}{1+n_{\text{th}}}\right)^n \prod_{k=1}^{n}\left(1+\frac{N_{\text{ex}}A_k}{kn_{\text{th}}}\right), \tag{3}$$

where $A_k = \sin^2(\Omega\sqrt{k}t_{\text{int}})$ is the emission probability for a single atom interacting with the cavity field. In these formulae, n_b is the thermal photon number, N_{ex} the normalized pump rate given by the atomic rate R, divided by the cavity lifetime τ, Ω the vacuum Rabi frequency and C a normalization constant.

3. Experimental set-up

A simplified experimental set-up is shown in figure 1. An atomic oven provides two collimated beams of rubidium atoms, one provides atoms for the main experiment and the second is used as an auxiliary reference beam for locking the laser (not shown in the figure). A frequency-doubled dye laser at a wavelength of $\lambda = 297$ nm is used to excite ^{85}Rb atoms of the atomic beam in a single-step transition from the $5S_{1/2}$ ($F = 3$) ground state to the $63P_{3/2}$ Rydberg state. The maser transition used in all of these experiments is a microwave transition between the Rydberg levels, $63P_{3/2}$ excited state and $61D_{5/2}$ ground state.

The heart of the micromaser is the superconducting niobium microwave cavity which has a closed cylindrical shape with length and diameter of about 2.5 cm. The cavity is cooled to below

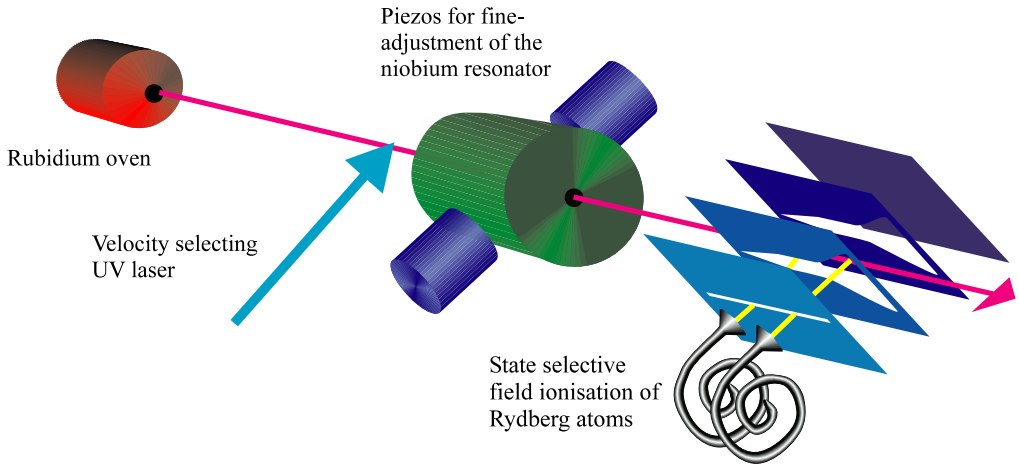

Figure 1. The experimental set-up. The atoms leaving the rubidium oven are excited into the $63P_{3/2}$ Rydberg state using a single-step UV excitation at an angle of 11°. After interacting with the cavity the atoms are detected using state-selective field ionization. Tuning of the cavity is performed using two piezo translators which squeeze the cylinder transversally. A reference beam stabilizes the laser to a Stark-shifted atomic resonance allowing the selected velocity subgroup to be changed continuously within the range of the velocity distribution of the atoms (this reference beam is not shown in the figure).

0.3 K by means of a ^{3}He–^{4}He dilution cryostat, leading to a mean thermal photon number of $n_{\rm th} = 0.03$. In a recent experiment a cavity with a Q factor of 4×10^{10} was produced with a field decay time of 0.6 s which corresponds to a photon lifetime of 0.3 s. The decay was measured using ring-down spectroscopy the result of which is presented in figure 2. This is the largest cavity Q factor ever obtained for this type of experiment and is more than two orders of magnitude larger than has been achieved in related experiments [17].

Each end of the cavity has a small centred bore with a diameter of about 3 mm. These holes are used as entrance and exit holes for the atomic beam and for coupling in external microwave signals for diagnostic purposes. The field mode used in the experiment is the TEM_{121} mode with a resonance at about 21.456 GHz. It can be fine-tuned by squeezing the cavity mechanically via two piezo translators.

The cavity Q factor is measured by observing the decay of a heterodyne beat signal obtained by mixing a seeded field that leaks out of the cavity with a local oscillator offset by 200 Hz. The result of such a measurement is shown in figure 2(A). Figure 2(B) is a Fourier transform of the decaying signal. This is centred at the 200 Hz beat frequency and has a width of 1.1 Hz. This is rather close to the homogeneous linewidth of the cavity (which is given by the decay time from figure 2(A)). This indicates that the cavity is relatively immune to frequency drifts over relatively long time scales. Small electric stray fields appear to be present at the entrance and exit holes of the cavity and are possibly caused by both contact potentials stemming from rubidium deposits in the holes and by single crystals of niobium that appear during the annealing of the cavities [6, 7]. These stray fields Stark detune the atoms reducing the effective length of resonant interaction by an small amount δL. This results in a lowered effective coupling strength $\Omega_{\rm eff} = (1/L) \int_{0+\delta L}^{L-\delta L} \Omega(x)\, {\rm d}x$. Thus, the effective coupling constant varies from experiment to

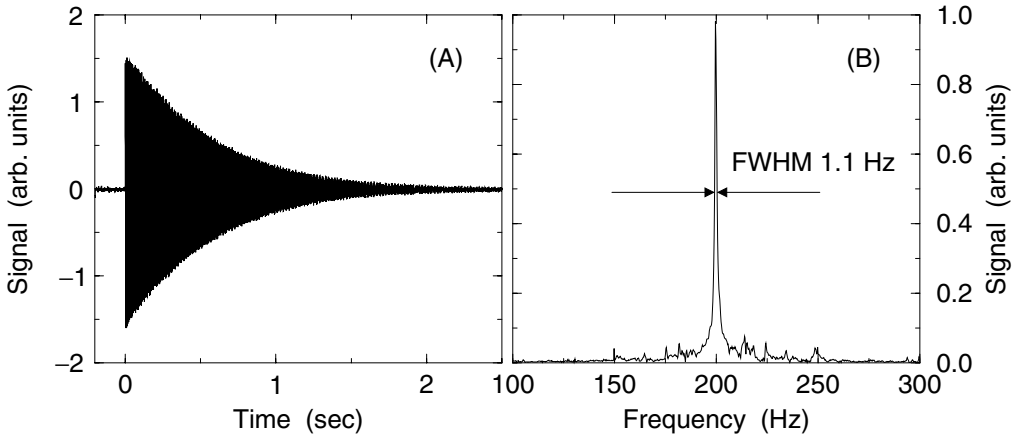

Figure 2. The cavity decay time is measured by ring-down spectroscopy. (A) The ring down of the beat frequency between the field leaking out of the cavity and a local oscillator offset by 200 Hz. (B) The Fourier transform of this signal showing a narrow 1.1 Hz wide peak.

experiment and must be calibrated for accurate knowledge of the Rabi frequency. Trapping states (see below) are now routinely used to gain highly accurate calibrations of Ω_{eff}.

The atomic beam is provided by an oven that is collimated to provide two atomic beams. One is directed into the main chamber and the other is an auxiliary beam (not shown), which is used as a frequency reference for locking the laser. Velocity selection of the atomic beam is achieved by exciting the atoms to the Rydberg state using a laser frequency detuned below resonance of the $5S_{1/2}$ ($F = 3$) to $63P_{3/2}$ resonance of ^{85}Rb with a laser that is angled towards the atomic beam at an angle of 11° to the normal. Thus, the only atoms excited are those for which the Doppler shift matches the frequency detuning of the laser. Frequency stabilization and locking of the laser is achieved via the auxiliary beam. Once the laser is locked to the auxiliary beam, tuning of the laser is realized by Stark shifting the atomic resonance in the auxiliary beam via a stabilized voltage to two electrodes at the excitation zone. The velocity of the Rydberg atoms passing through the cavity can be tuned continuously by simply changing the voltage of the Stark electrodes. In our set-up we can tune the interaction time from 30 to 160 μs. However, below 40 μs the Doppler distributions of the $63P_{1/2}$ and $63P_{3/2}$ levels overlap. The $63P_{1/2}$ do not interact with the cavity field but are detected in the field ionization zone thus leading to a disturbance in the atom statistics. The velocity selector is calibrated using time-of-flight measurements. The width of the time-of-flight peaks show that our velocity selectivity is better than 3%.

Since single microwave photons cannot themselves be readily detected, all the information about the field from the states is gained from the atoms emerging from the cavity. We detect the state of the atoms by a method of state-selective field ionization, as described in [18]. The atomic beam passes between two grounded plates along a long slit with increasing width along the path of the atoms. A static electric field is supplied by two electrodes outside the grounded plates causing an increasing field strength along the path of the atoms. Since the ionization potential of the upper maser level is smaller than the potential of the lower maser level, atoms in different states are ionized at different positions along the beam path. The electrons released are detected with a separate channeltron for each state. The signals are then converted into TTL

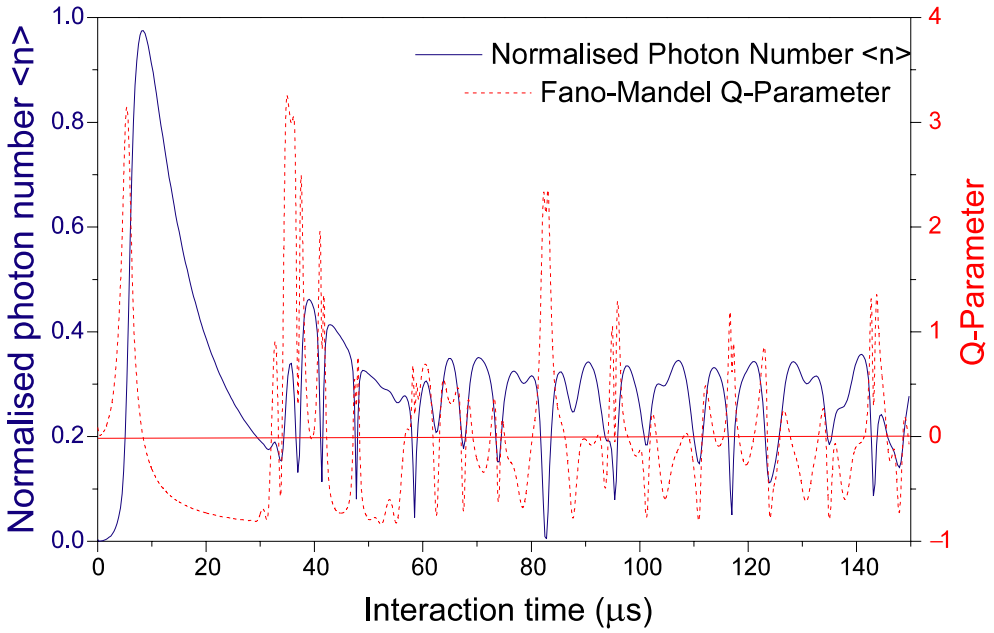

Figure 3. Dependence of the photon number on the interaction time. This is a pump curve for $N_{ex} = 20$ and a thermal photon number of 10^{-4} (or 100 mK). Also shown is the corresponding photon statistics. Movie 1 shows the appearance of trapping states as the temperature is reduced.

pulses. The state selectivity of our setup is about 5% miscounts in each of the channels at a total detection efficiency of up to $(40 \pm 10)\%$ although these numbers can vary depending on the specific voltages used and the alignment of the detectors. Miscounts in a specific detector can be made arbitrarily small at the expense of detector efficiency and higher miscount probabilities in the complementary detector.

4. Trapping states: steady state number states

Trapping states are the steady-state features of the maser field peaked at particular photon numbers and occur in the micromaser as a direct consequence of field quantization in a cavity. At low cavity temperatures the number of blackbody photons in the cavity mode is reduced, thus the influence of the emission probability dominates and trapping states begin to appear [10] (see figure 3 and Movie 1). Specifically trapping states occur when the atom field coupling, Ω, and the interaction time, t_{int}, are chosen such that in a cavity field with n_q photons each atom undergoes an integer number, m, of Rabi cycles. This is summarized by the condition,

$$\Omega t_{int}\sqrt{n_q + 1} = m\pi \tag{4}$$

for the trapping state denoted (n_q, m). When equation (4) is fulfilled, the cavity photon number is left unchanged after the interaction of an atom and hence the photon number is 'trapped'. This will occur regardless of the atomic pump rate N_{ex}. A trapping state is characterized by the upper-bound photon number n_q and the number of integer multiples of full Rabi cycles m. Trapping states are a dominant effect in the operation of the micromaser at low temperatures.

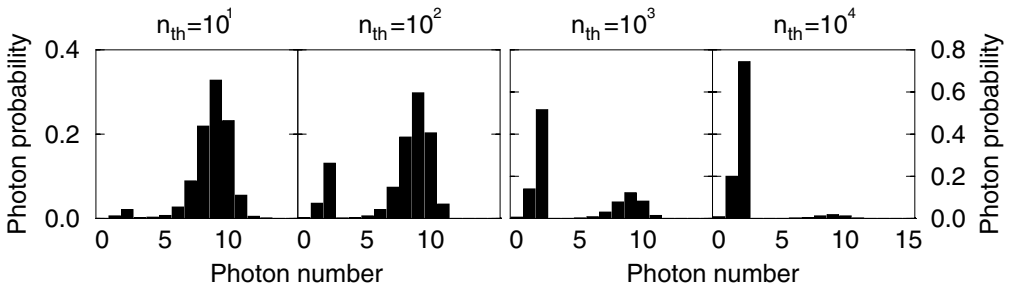

Figure 4. This simulation shows the effect of thermal photons on the steady-state photon number distribution ($N_{ex} = 25$). Movie 2 shows the effect of thermal photons for a wide range of interaction times, which includes many trapping states. The effect of thermal photons can be readily observed.

Movie 2 shows a 3-D plot of the photon number distribution in the micromaser over a wide range of interaction times, the near-Fock state photon distribution at the trapping states can be readily distinguished. The paper by Brattke *et al* [12] shows the accuracy of the theoretical treatment of micromaser theory by comparing theory and experiment for a wide variety of atom-cavity detunings and interaction times for which trapping states can be found. A detailed discussion of the effects of the trapping condition on the evolution of the micromaser field can also be found in [12]. In the following discussion we will concentrate on the effects of thermal photons as they represent the major obstacle in the ability to create trapping states. Following this discussion we present a method of overcoming the shortfalls of high thermal photon numbers. Thus the ability to generate Fock states of the field is increased by expanding the applicability of trapping states to a wider range of operating conditions. This result is contrary to the established requirements of trapping states where it is normally assumed that highly stable conditions and low thermal photons are required. While this is certainly true for the CW case, in a pulsed operation a significant improvement in stability can be obtained.

Under normal CW conditions in the micromaser, blackbody radiation at finite temperatures means that there is a small probability of having a thermal photons enter the mode. The presence of a thermal photon in the cavity disturbs the trapping state condition, and atoms can again emit photons. This causes the field to jump above the photon number n_q and a cascade of emission events will follow. This results in a build up of a new photon distribution with an average photon number $n > n_q$ (figure 4). Movie 2 shows the dependence of cavity temperature and interaction time on the micromaser photon number distribution. This movie impressively shows the build up of the trapping states as one makes the transition from high- to low-temperature operation.

The first trapping states in the maser field were reported in [10]. The results show a good qualitative agreement with the Monte Carlo simulations presented in [19]. As the arrival times of the ground state atoms was also collected in this experiment, it was also possible to extract the counting statistics of the ground state atoms leaving the cavity.

4.1. Trapping state stabilization

Trapping states are self-stabilizing, in that any photon loss due to cavity decay is replaced by a new photon from the pump atoms and when the cavity field is in the trapping state, the field distribution is localized to a single Fock state, where it will remain for a time determined by the

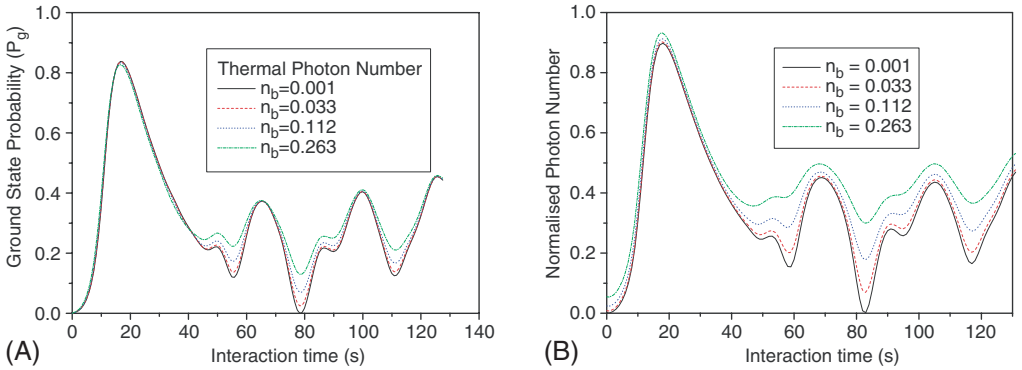

Figure 5. Theoretical simulation of the normalized photon number versus interaction time for a micromaser under normal operating conditions. (A) The CW photon distributions for the atom rate of 750 atoms s^{-1} during a pulse corresponding to a time average pump rate 250 atoms s^{-1}. (B) Same plot for the unpulsed (CW) normalized photon number for an atomic rate of 250 atoms s^{-1}. The improvement in visibility introduced by pulsing the laser is quite clear.

rate of entry of thermal photons into the cavity. As we have shown above, thermal photons destroy the trapping condition. Thus the best stability is achieved by adding a new loss mechanism that can remove any build up of a field beyond the trapping state. This could either be by adding lower state atoms to the beam (ground states in the trapping states) or a feedback mechanism that reduces the pump rate to compensate for increased emission [20].

However, a simpler and ultimately highly effective method is to operate the micromaser in cyclic operation, where the pump atoms are turned on and off for short periods (in comparison with the rate of the build up of the thermal field) for pump and relaxation cycles. During the pumping cycle the cavity begins to fill with photons, approaching the CW conditions, the pump rate is turned off for a period to allow the field to relax a little before the next pumping cycle, thus correcting for the entry of thermal photons and allowing the field to build up back to the trapping condition in the next pulse. After many such cycles the field reaches a steady state, which is a combination of the pumping cycle and the relaxation cycle. In this mode of operation, the entry of thermal photons only affects a single pulse after which the cavity is allowed to relax to a photon number below the steady-state value. Under this operation, trapping states are a dominant feature of micromaser dynamics for a wide range of pump rates and thermal photon numbers.

The theoretical model for calculating the cyclically steady state of the maser (the steady state produced for a pulsed pump cycle) was developed to calculate photon distributions for the analytical analysis of Fock states in the experiment presented below and can be found in [14]. Figure 5 shows two sets of theoretical plots of the normalized average photon number ($\langle n \rangle / N_{\mathrm{ex}}$) versus interaction time (T_{int}) for cyclic and CW operation of the micromaser for a series of thermal photon numbers, corresponding to temperatures from 100 mK to 1 K. The cyclic pulse widths were chosen to be $t = \tau_{\mathrm{cav}}/3$ pump time with $t = \tau_{\mathrm{cav}}$ between pulses. As this is a one-third pump cycle, the atomic rate during the pump cycle for the cyclic operation was set accordingly in order to maintain the same long term time average rate as with the CW theory. In this way we compare like with like and indeed for low-temperature behaviour both plots are identical, it is only as the temperature of the cavity is increased that the difference becomes quite remarkable.

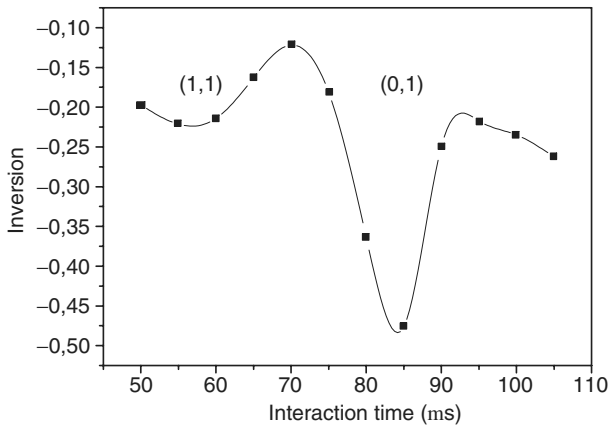

Figure 6. Experimental realization of trapping states occurring in the cyclically steady-state micromaser. It is easy to see that in comparison with the results of Weidinger *et al* [10] the trapping states have a very high visibility. This is an important result as it shows that trapping states are much more stable than has ever been predicted and could readily be observed even in systems that are less suitable for the observation of CW trapping states.

In figure 5(A) the visibility of trapping states (which show up as dips in the curve) remain almost unaltered whilst they lose visibility rapidly in figure 5(B).

In calculating these plots, additional effects such as interaction time averaging and detuning fluctuations have not been included in the theoretical calculations. The intention here was to show that in the cyclically steady-state trapping states are a more robust feature. This remains true even in the face of increased fluctuations.

We performed this experiment and present the results of this test here for the first time. Figure 6 shows an experimental plot of trapping states that is obtained when the cyclically steady state is used, which when compared with the results of Weidinger *et al* [10] is a substantial improvement in visibility.

The consequences of this are that pulsed operation allows us to find trapping states with greater ease than has ever been previously suspected. This enables us to calibrate an experimental apparatus that is operated under conditions in which trapping states would never have been suspected to be present and is now routinely used to calibrate the vacuum Rabi frequency at the start of experimental scans. This also shows us how trapping states can be used to stabilize a cavity field and produce Fock states on demand [12, 15] (see below). The ease with which this method enables us to find trapping states has allowed us to make use of these states to perform accurate calibrations of the apparatus, thus significantly improving our ability to operate the micromaser.

5. Observation of $|n\rangle$-photon number states in a cavity

In the normal mode of operation, a micromaser field develops solely due to the action of single atoms interacting with the field of a single-mode cavity. Once having interacted with the field, the atom is detected in excited or ground state by a state-selective field ionization. This occurs with a 40% detection efficiency and a 5% miscount rate. The miscount rate can be made arbitrarily low for a single detector with a small trade off in the total detection efficiency. When the atoms

leave the cavity in a micromaser experiment they are in an entangled state with the field; hence an EPR relationship can be used to determine the field state. This is known as state reduction and was proposed by Krause *et al* [21] as a method of observing the buildup of the cavity field to a known Fock state. More formally, if the cavity field is initially in the state $|n\rangle$, the interaction of an atom with the cavity leaves the cavity field in a superposition of the states $|n\rangle$ and $|n+1\rangle$ and the atom in a superposition of the internal atomic states $|e\rangle$ and $|g\rangle$. Thus the state of the atom–field system becomes

$$\Psi = \cos(\phi)|e\rangle|n\rangle - \mathrm{i}\sin(\phi)|g\rangle|n+1\rangle, \tag{5}$$

where ϕ is a phase acquired by the atom–field system due to Rabi oscillations in the cavity. The state-selective field ionization measurement of the internal atomic state reduces the field to one of the states $|n\rangle$ or $|n+1\rangle$. State reduction is independent of the interaction time, hence a ground state atom always projects the field onto the $|n+1\rangle$ state independent of the time spent in the cavity. This results in an *a priori* probability of the maser field being in a specific but unknown number state [21]. If the initial state is the vacuum, $|0\rangle$, then a number state created is equal to the number of ground state atoms that were collected within a suitably small fraction of the cavity decay time.

Experimentally the presence of Fock states in the cavity is verified using a pump-probe experiment, in which a pump atom (or atoms) prepares a quantum state in the cavity and the Rabi phase of the emerging probe atom measures the quantum state of the cavity field. The signature that the quantum state of interest has been prepared is simply the detection of a predefined number of ground-state atoms. To verify that the correct quantum state has been projected onto the cavity mode, a probe atom is sent into the cavity with a variable but well-defined interaction time. Rabi oscillations of the probe atom reveal the state of the cavity field through the relationship (2). As the formation of the quantum state is independent of the interaction time we need not change the relative velocity of the pump and probe atoms, thus reducing the complexity of the experiment. This experiment reveals the maximum amount of information that can be found relating to the cavity photon number and is in a sense related to the 'endoscopic measurement' proposed by Bardoff *et al* [22]. We recently used this method to demonstrate the existence of Fock states up to $n = 2$ in the cavity using the method presented in [13], where the experimental apparatus (figure 1) and data collection methods were described in detail. The results are reproduced here in figure 7. Briefly, the Rydberg atoms were prepared using very short laser pulses, thus ensuring that a detection of n ground-state atoms truly represented n photons in the cavity with a high probability. As there is typically a delay of 1–2 ms between the preparation atoms and the probe atom, some dissipation due to the finite lifetime of photons in the mode (25 ms in this case) will occur. Thus the most realistic fit to the data is obtained with equation (2). The histograms on the right-hand side of figure 7 show the coefficients P_n obtained from fitting this equation.

The use of equation (2) implies that the cavity mode is quantized; however it is interesting to note that equation (1) is still a good fit to the data. A comparison between the Rabi frequency Ω extracted using equation (1) and the theoretical frequency variation expected for a Fock state was made in [13]. This is reproduced here as figure 8. The photon number n is not an element of this fit, hence the Rabi frequency is an unrestricted classical variable. This simple fit, however, remains a good approximation because the decay of the photon number state is quantized; thus, the probe Rabi oscillation is dominated by the initial Fock state for short times following the creation of the state (figure 8). If, on the other hand, the state was decaying classically, the Rabi

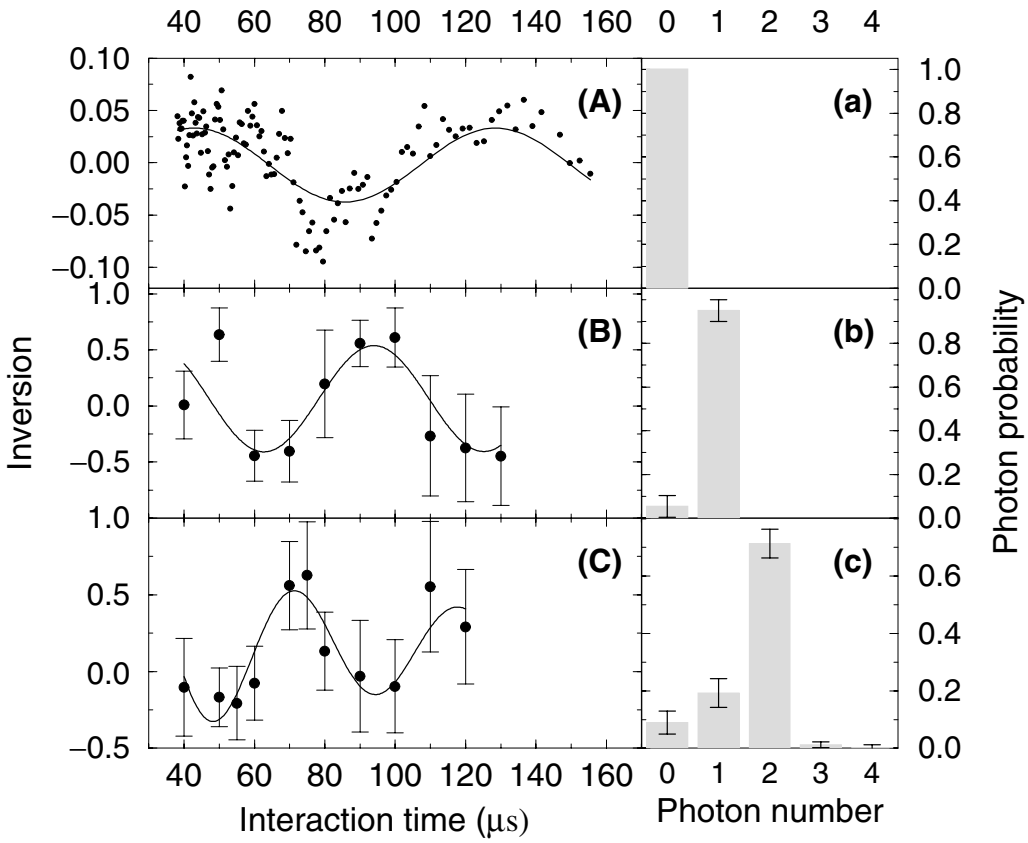

Figure 7. (A)–(C) Three Rabi oscillations are presented, for the Fock state $n = 0, 1$ and 2. (a)–(c) Plots presenting the coefficients P_n resulting from fits to equation (2). In each fit there is a clear maximum photon number which corresponds to the target Fock state.

frequency would also change classically with a smooth variation from $n = 2$ to $n = 0$, with the caveat that we are already speaking of quantum states having no classical analogue. Given the photon distribution measured in figure 7, the Rabi frequency for a classical decay can be calculated. This is marked as a square above the $n = 2$ position in this graph. Thus we have observed a significant departure from the classical decay of a cavity mode, indicating that the field can only decay in units of a single photon.

The observation of Fock state Rabi oscillations is also interesting as it is the first direct observation of the atom–field interactions that are fundamental to the Jaynes–Cummings Hamiltonian (figure 7). It is therefore the case that all of the physics of the steady-state operation of the micromaser can be produced from combinations of these three plots up to a photon number of $n = 2$. One consequence of the emission probabilities dependence on the photon number n is that the detection of an atom in the excited or ground state affects the emission probability all following atoms by changing the photon number in the cavity. Correlated emissions in the steady-state micromaser operation have been discussed previously [8] and can be observed in figure 7 where significant changes in the emission probability of a probe atom result from the emission of preceding atoms. In the one-photon Rabi oscillation, for example, the sequence of atoms reaches correlations up to 75%, changing from highly correlated emission to highly anti-correlated emission as a function of interaction time. That the correlation is not 100% can

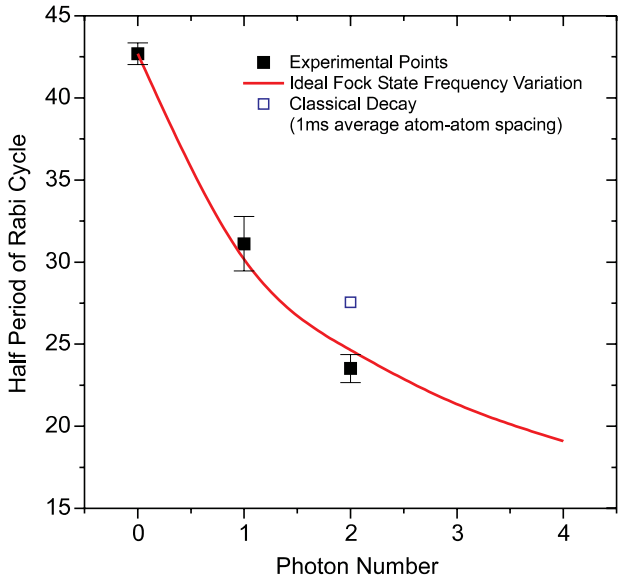

Figure 8. Dependence of the Rabi frequency on the photon number. A single sine fit to each of the three curves 2 A, B, C, is plotted versus the theoretical variation of frequency as a function of photon number. The coupling constant 36.8 krad s^{-1} is the optimum fit to the data.

be attributed to dark counts and fluctuations in experimental parameters, the single-frequency Rabi oscillation indicates the true correlations could be as high as 95%.

The usefulness of figure 7 as a description of the steady-state micromaser does not end at this point as trapping state, sub-Poissonian field statistics and collapse and revival of Rabi mutations are all contained in this picture. For example, when the interaction time corresponding to the trapping state condition is met, i.e. when the emission probability A_k is zero or $\Omega\sqrt{k}t_{\rm int} = k\pi$, the formation of the cavity field is identical to that which occurs in the steady state and the probe atom will perform an integer number of Rabi cycles. One would therefore expect that the measured photon number distribution, in the dynamical measurement of Varcoe *et al* [13], would be the same as that predicted for the trapping states for the equivalent pump rates. Figures 9 and 10 show the relationship between these two conditions along with an analytical calculation of the expected photon distribution. The details of the analytical calculation will be presented elsewhere [14], briefly, we make a few idealizing assumptions: thermal photons are only taken into account for the long-term buildup of the cyclically steady state and Gaussian averaging over velocity spread of atoms of about 3%. Considered in the calculations are the exponential decays for the cavity field during the pulse when either one (for $n = 1$) or two photons were deposited one by one (for $n = 2$) changing the photon number distribution. The simulations also average over the Poissonian arrival times of the atoms; see [14] for details. The results of these calculations are compared with the experimental results in figures 11(a) and (b), respectively.

6. Single photons on demand

As they are the ultimate quantum resource, a source of Fock states on demand is one of the driving forces behind many experiments in quantum optics today. Recently, we have demonstrated a

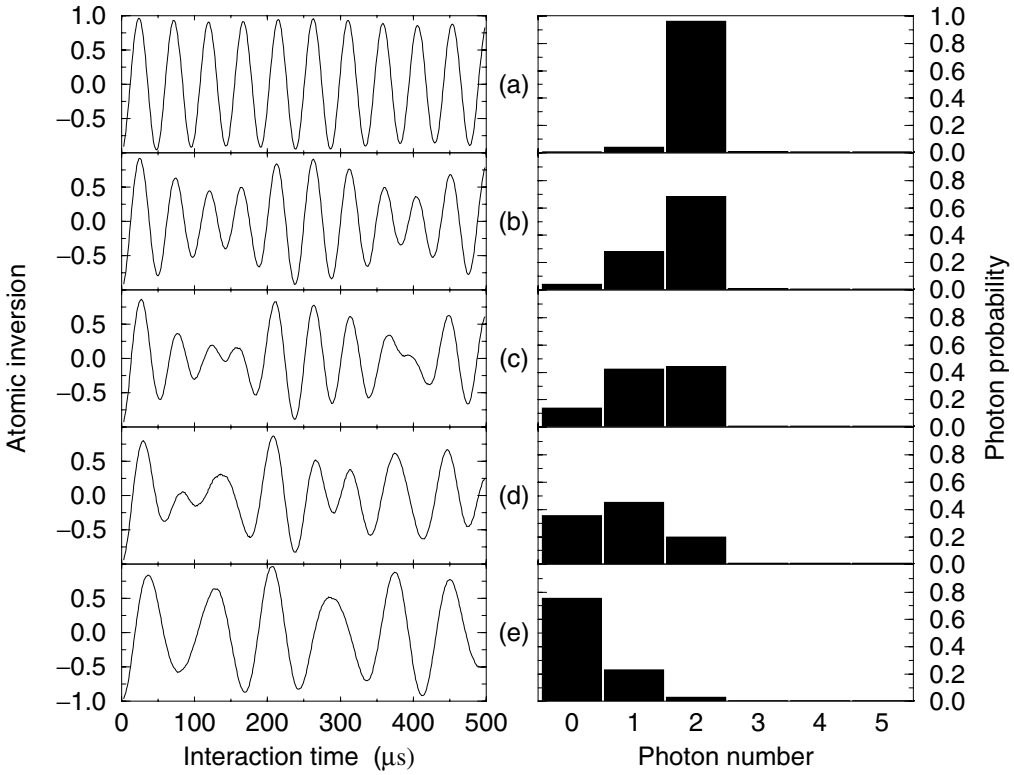

Figure 9. This figure shows Rabi oscillations (left) experienced by a probe atom at various time intervals after the creation of a two-photon Fock state. After creation and in the presence of dissipation, the Fock state decays (right) finally ending up in the ground state after a long time delay. If this was a classical decay, the frequency of the Rabi oscillations would smoothly vary from top (a) to bottom (e). This is pictured in figure 10. Quantum mechanical decay, on the other hand, is dominated by the original Fock state for the initial portion of the decay (b), with the frequency of oscillation determined by equation (1).

source of not only single photons, but of arbitrary Fock states *on demand*. They are created in the cavity and on a time scale of less than $0.1\tau_{\mathrm{cav}}$. All sources which use a cavity are restricted to using cavity decay as the means of allowing the created photon to escape, and this experiment is identical in that respect; we are however quite fortunate in that the cavity decay time is quite long and therefore the Fock state remains to interact with probe atoms.

To demonstrate the principle, figure 12 shows a simulation of a sequence of 20 pulses of the pumping atoms, in which an average of seven excited atoms per pulse are present. Two operating conditions are presented comparing conditions outside trapping conditions ($\Omega t_{\mathrm{int}} = 1.67$) with the (1,1) trapping state ($\Omega t_{\mathrm{int}} = 2.2$). Below the pulse sequences, two distributions show the probability of finding 0 to 5 atoms (and hence photons) per pulse in the cavity. Under the trapping condition only a single emission event occurs, producing a single lower state atom which leaves a single photon in the cavity. Since the atom–cavity system is in the trapping condition, the emission probability is reduced to zero and the photon number is stabilized. The variation of the time when an emission event occurs during the atom pulses in figure 12 is due to the Poissonian spacing of upper-state atoms entering the cavity and the stochasticity of the quantum process.

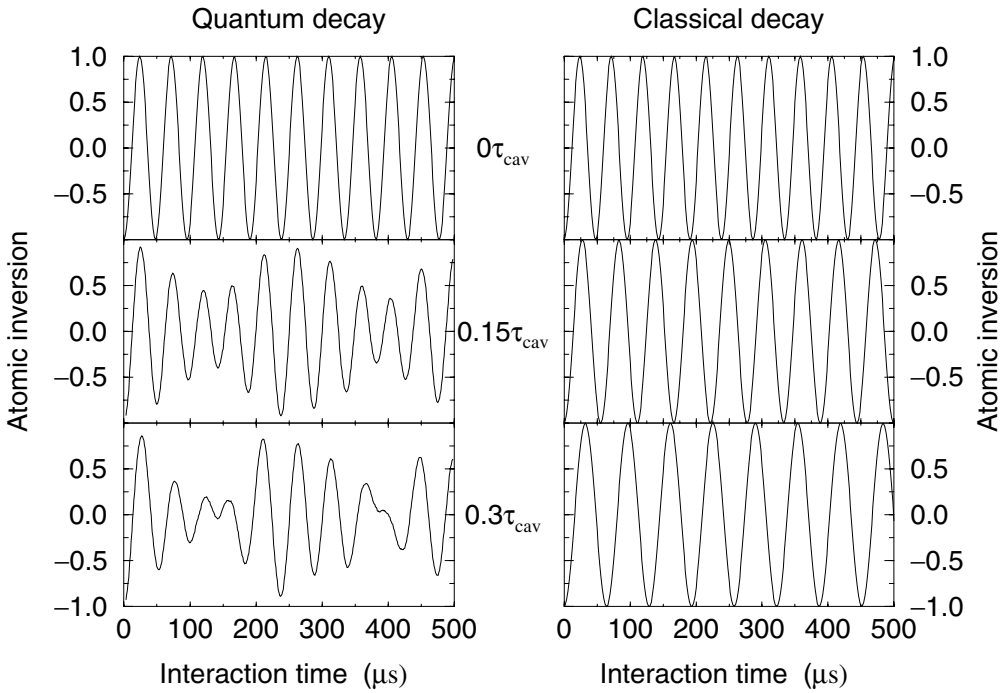

Figure 10. This figure shows a comparison of quantum decay to a completely classical decay of the cavity field for short times following the creation of the state. The middle panel corresponds to the approximate time between the creation of the state to the time of measurement. The predicted period of oscillation of the middle panel is used to plot the position of classical decay in figure 8.

In figure 12(A) the broader photon number distribution is due to the absence of a feedback stabilization.

The variation of the time when an emission event occurs during an atom pulse in figure 12(A) is due to the variable time spacing between the atoms as a consequence of Poissonian statistics and the stochasticity of the quantum process. The atomic rate therefore has to be high enough that there will be a sufficient number of excited atoms per laser pulse, in order to maintain the 98% probability of an atom emitting.

Figures 13(a) and (b) show the probability of single-photon Fock state creation as a function of the average number of atoms per pulse for the (1,1) and (1,2) trapping states. The (1,2) trapping state (figure 13(b)) shows a faster approach to the Fock state than for the (1,1) trapping state. For a given cavity photon number the probability of emission into the cavity is given by

$$P_g = \sin^2(\sqrt{n+1}\Omega t_{int}). \tag{6}$$

The faster rise time of the (1,2) trapping state can therefore be attributed to the higher emission probability into the empty cavity (or vacuum) of 92.9% as compared with the emission probability at the position of the (1,1) trapping state being 63.3%. The (1,2) trapping state therefore appears to be the better position for single-photon Fock source operation, but if the trapping condition is violated by a thermal photon or other fluctuations, a higher stability is achieved when the $n + 1$ emission probability is small. Thus although the (1,2) trapping state is slightly

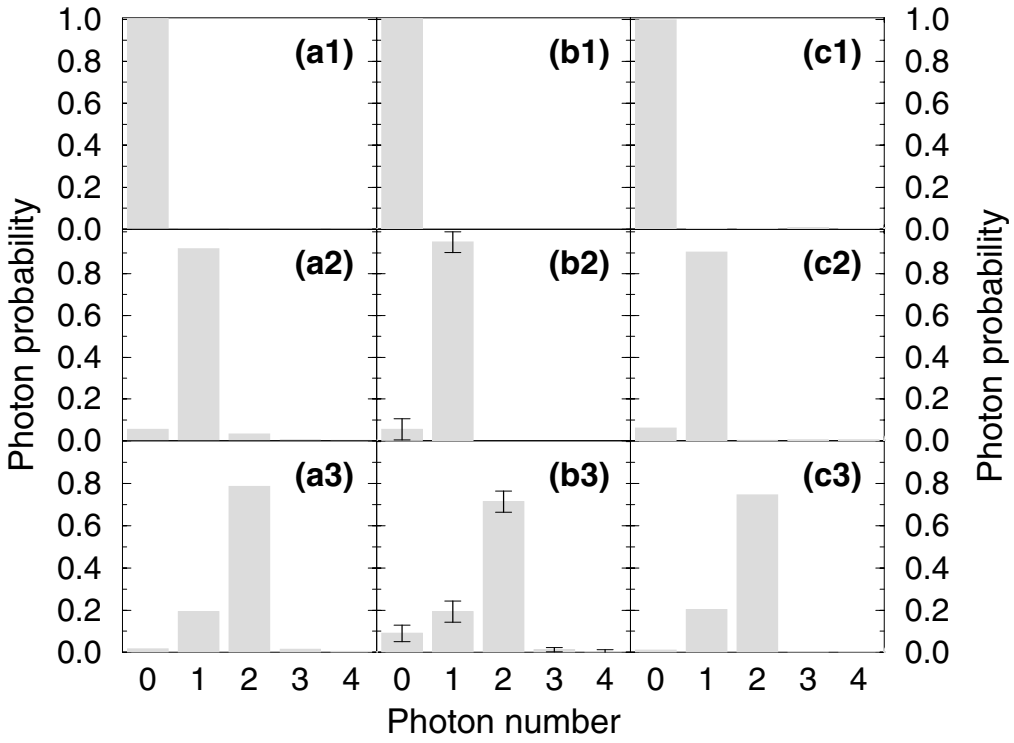

Figure 11. Comparison between theory and experimental results on the purity of Fock states. The columns represent photon distributions obtained from; (a) a theoretical simulation of the current experiment; (b) the current experimental results; and (c) a theoretical model that extends the current experiment to the steady state at the positions of the trapping states. The agreement between these three results is remarkable, indicating that dissipation is the most likely loss mechanism. Vertically the plots refer to the three Rabi oscillations $n = 0, 1, 2$ from figure 7.

more favourable for small average atom numbers, it is more unstable at higher average atom numbers and the (1,1) trapping state reaches a higher total probability of single-photon Fock state creation (see figure 13). The change of the emission probability as a function of the photon number n by a single quantum thus has an appreciable effect on the evolution of the system. This discussion acquires more relevance when the creation of Fock states $\geqslant 2$ is considered.

There is an upper bound to the probability of finding exactly one lower state atom per pulse, which is governed by the emission probability and the Poissonian distribution of atoms. This maximum probability is given by

$$P^{\max} = 1 - \mathrm{e}^{-P_{\mathrm{g}} N_{\mathrm{a}}}, \tag{7}$$

where N_{a} is the average number of atoms per pulse and is the most important factor when comparing different operating conditions. A critical value of N_{a} can be defined that can be considered a threshold pump rate. We define the threshold pump rate to be $N_{\mathrm{Thr}} \equiv 2/P_{\mathrm{g}}$ leading to a threshold of $N_{\mathrm{Thr}} = 3.16$ for the (1,1) trapping state and $N_{\mathrm{Thr}} = 2.15$ for the (1,2) trapping state.

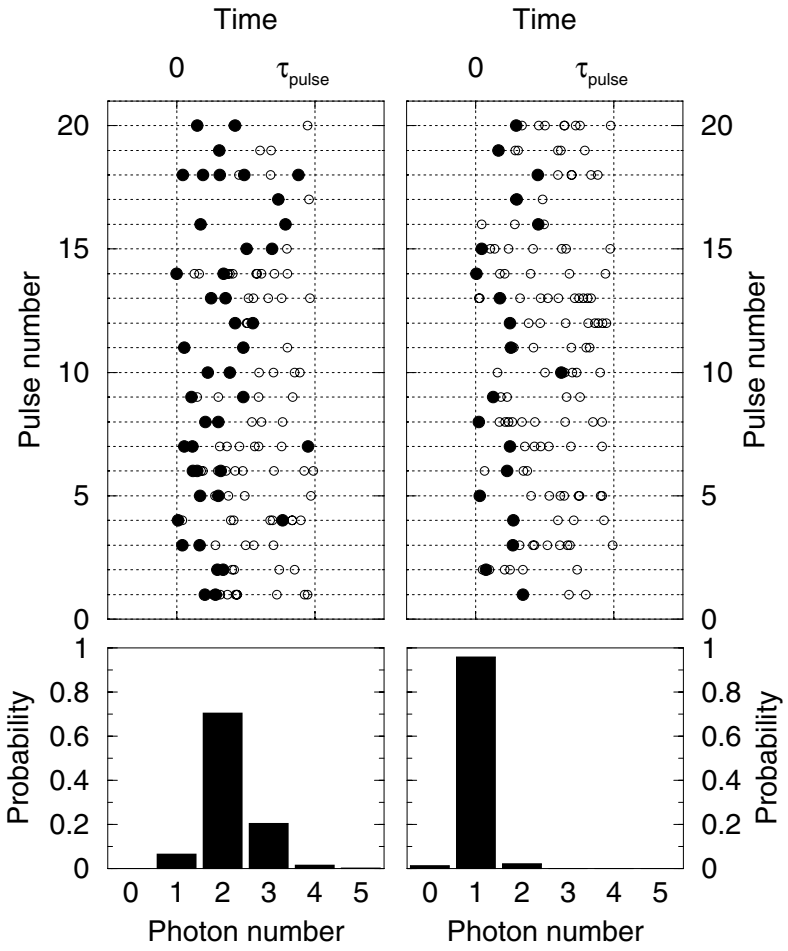

Figure 12. This figure shows a simulation of a subset of 20 subsequent pulses of the excitation laser and the associated probability distribution for photons or lower state atom production (●, lower state atoms; ○, excited state atoms). The start and finish of each pulse is indicated by the vertical dotted lines marked 0 and τ_{pulse}, respectively. The two operating conditions are (left) outside the trapping state conditions ($\Omega t_{\text{int}} = 1.67$) with a broad-field distribution; and (right) the (1,1) trapping state ($\Omega t_{\text{int}} = 2.2$) with a near Fock state distribution. Both distributions are sub-Poissonian but they are readily distinguishable experimentally. The size of the atoms in this figure is exaggerated for clarity. With the real atomic separation there are 0.06 atoms in the cavity on average (i.e. well into the one-atom regime). The other parameters are $\tau_{\text{pulse}} = 0.02\tau_{\text{cav}}$, $n_{\text{th}} = 10^{-4}$ and $N_{\text{a}} = 7$.

To guarantee single-atom single-photon operation, the duration of the preparation pulses must be short in relation to the cavity decay time. For practical purposes, the pulse duration should be smaller than $0.1\tau_{\text{cav}}$ for dissipative losses to be less than 10%. Apart from reducing the fidelity of the Fock state produced, losses increase the likelihood of a second emission event leading to larger number of lower state atoms than photons in the field, whereby the 1 : 1 correspondence between both would be lost. Shorter atom pulses reduce the dissipative loss; however the number of atoms per cavity decay time (usually labelled N_{ex}) must be larger than

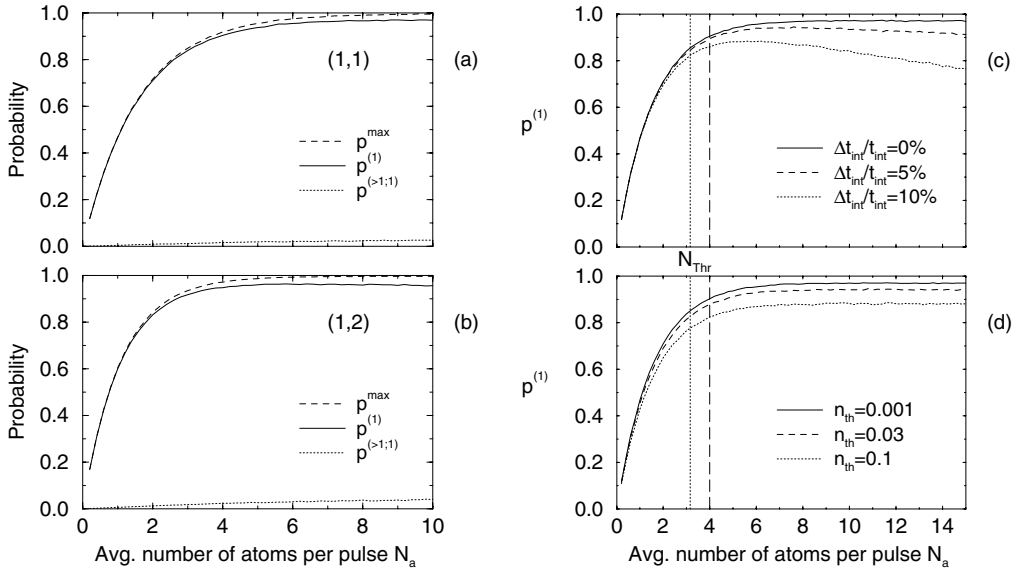

Figure 13. (a), (b) A comparison for one-photon Fock state generation under the conditions of the (1,1) and (1,2) trapping states. Higher emission probability into the vacuum for the (1,2) trapping state means a faster approach to the operation of an unconditional single-photon Fock source. However, violation of the trapping conditions by a thermal photon causes higher emission at high pump rates, implying that the (1,2) trapping state is more vulnerable. The (1,1) condition therefore reaches a higher final Fock state creation probability. The conditions for this simulation are $\tau_{\mathrm{cav}} = 100\,\mathrm{ms}$, $\tau_{\mathrm{pulse}} = 2\,\mathrm{ms}$ and $n_{\mathrm{th}} = 10^{-4}$. (c), (d) Demonstrates the robustness of the unconditional Fock source. Presented here is the probability of finding exactly one atom per pulse ($P^{(1)}$) for a range of experimental conditions. (c) Robustness of the Fock source against (c) interaction time averaging and (d) as a function of temperature. It should be emphasized that the upper level of vibrations and thermal photons considered in this figure are extreme conditions and very much higher than those of a typical experiment. Experimental parameters of ($n_{\mathrm{th}} = 0.03$, $\Delta t_{\mathrm{int}}/t_{\mathrm{int}} = 0.02$) are well within these limits. The threshold, N_{Thr}, for Fock state operation (dotted vertical line) and the pump rate, N_{a}, attained in our present experiment (broken vertical line) are both indicated on the figure.

$10N_{\mathrm{Thr}}$ to realize the Fock source with a significant fidelity. Since a minimum atom number is required to produce the desired state, care must also be taken to avoid atom beam densities violating the one-atom-at-a-time condition.

For a large range of operating conditions, the production of Fock states of the field and single lower state atoms is remarkably robust against the influence of thermal photons, variations of the velocity of atoms and other influences such as mechanical vibrations of the cavity. Much more so than the steady-state trapping states, for which highly stable conditions with low thermal photon numbers are required [10, 13]. Figures 13(c) and (d) show the probability of finding exactly one atom in the lower state per pulse ($P^{(1)}$) for an extreme range of interaction time spread and increased thermal photons. This robustness results from the relatively short preparation pulse

($\leqslant 0.1\tau_{\rm cav}$) which prevents external influences from greatly affecting the generation of Fock states. In addition, when fluctuations do occur they affect only a single experimental iteration after which the cavity is reset to the vacuum. It must be emphasized that the upper limit of fluctuations considered in figures 13(c) and (d) is well above that of a typical experiment and the routinely used experimental parameters of $n_{\rm th} = 0.03$ ($T = 300\,{\rm mK}$) and $\Delta t_{\rm int}/t_{\rm int} = 2\%$. Here we require high pumping rates ($N_{\rm ex} \geqslant 40$) and as a consequence the steady-state operation of the micromaser would not exhibit trapping states, but even at these extreme conditions, the simulation shows that under pulsed excitation the system still acts as an effective single photon Fock source. It is therefore possible that this Fock source is generalizable to a wide variety of systems including related systems for optical radiation [23].

An obvious side effect of the production of a single photon in the mode is, as mentioned already, that a single atom in the lower state is produced. This atom is in a different state when it leaves the cavity and is therefore distinguishable from the pump atoms, hence under this operation, the micromaser also serves as a source of single atoms in a particular state, a requirement for many proposed experiments.[4–6]

Although the distribution of lower state atoms leaving the cavity will be maximally sub-Poissonian, the arrival time of an atom within the pumping pulse still shows a small uncertainty, the upper limit of which is determined by the pump pulse duration in the range of 0.01–$0.1\tau_{\rm cav}$ for the parameters used in this paper. The separation of the pulses is $\geqslant 3\tau_{\rm cav}$ leading to a small relative variation in the arrival times. If one would increase the pump rate still further, the pulse lengths could be further reduced and the arrival of an atom becomes even more predictable.

6.1. Photon Fock source: the experimental results

The present set-up of the micromaser was specifically designed for steady-state operation and is therefore not ideal for the parameter range presented here. However, the current set-up does permit a comparison between theory and experiment in a relatively small parameter range. The experimental test relies on the measurement of an absolute number of atoms and although the operation of the Fock source is independent of detector efficiencies, the experimental test is blurred by the fact that the state-selective field ionization detectors for the Rydberg atoms do not reach an efficiency of 100%. Atoms in a particular state will therefore be missed leading to wrong or misleading results. In order to circumvent this disadvantage, it is useful to measure population correlations between subsequent atoms instead. Owing to the strong coupling between the atoms and cavity, the cavity field and the state of the pumping atom are entangled following the interaction. A subsequent pumping atom will thereby also become entangled with any previous one; thus the population correlations between subsequent atoms are determined by the particular dynamics of the atom–cavity interaction. The connection between population correlations and the micromaser dynamics has been studied in detail in previous papers [8, 28]. It is important to

[4] The error tolerant quantum computing proposal by Gottesman and Chuang [24] requires that a 'quantum resource' be supplied *on demand* to facilitate computation. Such a source can be provided by the apparatus considered here; see [25].

[5] Sources of single atoms, such as the one described in this paper, are routinely employed for hypothetical tasks such as the creation of an atomic beam with arbitrary timing sequence or for the stabilization of cavity states; see e.g. [26].

[6] Proposals such as the teleportation of an atomic state using multiple atomic beams would be substantially enhanced when atoms arrive on demand rather than by chance; see e.g. [27].

note that even in the presence of lost counts, the correlations between subsequent detected atoms are maintained. Conditioning the experimentally measured parameter on the detection of atom pairs that contain at least one lower state atom, provides both a value appropriate to the existing correlation and—at the same time—directly related to the total probability of finding one atom per pulse.

By means of an extremely high cavity Q factor (4×10^{10}) an $N_{\rm ex}$ of approximately 60 atoms per cavity decay time was accessible for a short range of interaction times around the maximum in the Maxwell–Boltzmann velocity distribution, which happens to correspond with the interaction time for the (1,1) trapping state. A pulse length of $\tau_{\rm pulse} = 0.066\tau_{\rm cav}$ leading to an average of 4 atoms per pulse was chosen as a compromise between the effects of dissipation and external influences, while still providing a pump rate above the threshold for single-photon Fock state production. In the experimental data of Brattke *et al* [15] the ratio of two-atom events to the total number of two-atom events was evaluated that contain at least one lower state was evaluated. That is

$$P^{(>1;1)} = \frac{N_{\rm gg}}{N_{\rm gg} + N_{\rm eg} + N_{\rm ge}}, \tag{8}$$

where, for example, $N_{\rm eg}$ is the probability of detecting a two-atom event containing first an upper state atom (e) and then a lower state atom (g) in any given pulse. The number of three-atom events detected is negligible and can be effectively ignored as a contributing factor. Constructing the parameter in this way ensures that there is a one to one correspondence between the correlation parameter and the maximum probability of finding exactly one atom per pulse. That is, to a good approximation for pump rates and pulse durations employed in this experiment, the difference between the upper bound $P^{\rm max}$ and the measured correlation $P^{(>1;1)}$ gives the probability of finding exactly one atom per pulse ($P^{(1)}$). $P^{(>1;1)}$ in equation (8) is independent of the absolute detector efficiency and depends only on the relative detector efficiencies and the miscount probability (the probability that a given atomic level is detected in the wrong detector), each of which has been measured experimentally. As discussed in [15] the experiment shows that in at least 83.2% of the pulses a one-photon Fock state was created. Note that this is therefore the rate of single atom production and is in agreement with the observed probability of single lower state atom events when absolute detector efficiencies of approximately 40% are incorporated.

As the present apparatus was designed for operating the micromaser under steady-state conditions, the current results were obtained under extreme operating parameters of the apparatus and at an extreme cavity Q factor. However, this need not be the case. Future developments will incorporate the two improvements to increase the atomic flux and introduce a second pulse of atoms with variable velocity to act as a field probe. With these changes it will be easier to arrive at the optimum conditions for the Fock source and, in addition, will allow direct measurements of the cavity photon number by means of Rabi oscillations of the probe atom [13] and further studies of quantized field effects.

The source described here has the significant advantage over our previous method of Fock state creation [13] of being unconditional and therefore significantly faster in preparing a target quantum state. Previously, the state was prepared by the dynamics of the interaction of excited state atoms with the cavity field. State reduction occurred on detection of a lower state atom indicating the preparation of the desired cavity field. In the current experiment, however, the cavity field is correctly prepared in 83.2% of the pulses, independently of state reduction and hence atomic detection efficiency. Simply detecting the lower state atom as it

emerges from the cavity increases the fidelity of the one-photon Fock state to $\geqslant 95\%$ at the moment of detection (incorporating both dissipative losses and detector miscounts). Assuming 40% detector efficiency, detection of a lower state atom within any given preparation pulse will occur with a 37% probability. This should be compared with the 95% fidelity of the measured Fock state in [13], in which there was a $\leqslant 1\%$ probability of detecting the correctly prepared state. Thus along with the first observation of the operation of a single-photon Fock state source, we also have an order of magnitude improvement of Fock state creation over our previous experiment.

6.2. Extension to higher photon numbers

We shall now briefly consider the extension of Fock state creation to the creation of photon numbers greater than 1. There are two possibilities: the first is simply to operate in the trapping state corresponding to the required Fock state; the second is to build up the state one photon at a time by using a series of pulses.

To create a higher-order Fock state, one requires that the filling proceeds as fast as possible. High pump rates are therefore required. However as was noted above, in a real experimental situation, an optimum strategy must be employed to reduce losses and errors in the number of photons. The use of a single trapping state alone is therefore not the best procedure. The optimum strategy is to use the selectivity and self-stabilization provided by the trapping states to full advantage. Using the highest possible atomic flux one should start at the (1,1) trapping state to create the first photon, then build the field one photon at a time using a succession of pulses each one at the next highest trapping state. This is achieved by tuning each time to a different velocity sub-group until the target Fock state is achieved. This can be likened to climbing a photon ladder one rung at a time. Such a pulse sequence is depicted in figure 14, demonstrating that for realistic operating conditions, the Fock states up to $n = 4$ can be created with fidelities above 92%. The ideal conditions required for the multiple photon Fock source are still beyond that which can be achieved simply in the current apparatus, although twice the current atomic flux would already enable the creation of a two- or three-photon state with an excellent fidelity. In the near future, the operating conditions should be quite sufficient to surpass this limit.

7. Summary

We have reviewed three methods of creating Fock states in the micromaser: first using trapping states and secondly using state reduction of lower state atoms leaving the cavity to count the number of photons in the field mode. Finally, we present and experiment in which Fock states are created on demand in the cavity, this is the first to be able to produce the $n = 1$ state with a high level of reliability and repeatability and still remains the only experiment in principle capable of providing an arbitrary Fock state (at least up to $n = 4$) on demand. The benefits of this type of source to areas such as quantum communication, cryptography and computing are rather apparent. The stability and robustness of the source as well as the relative simplicity of its implementation suggest that the transfer to related optical systems [23], where Fock states can be made available for transmission between systems, is a distinct possibility. The knowledge of the quantum state of a system, its time of creation and expected arrival time, are vital to the secure and speedy transfer of information [29]. Distributed quantum computing, on the other

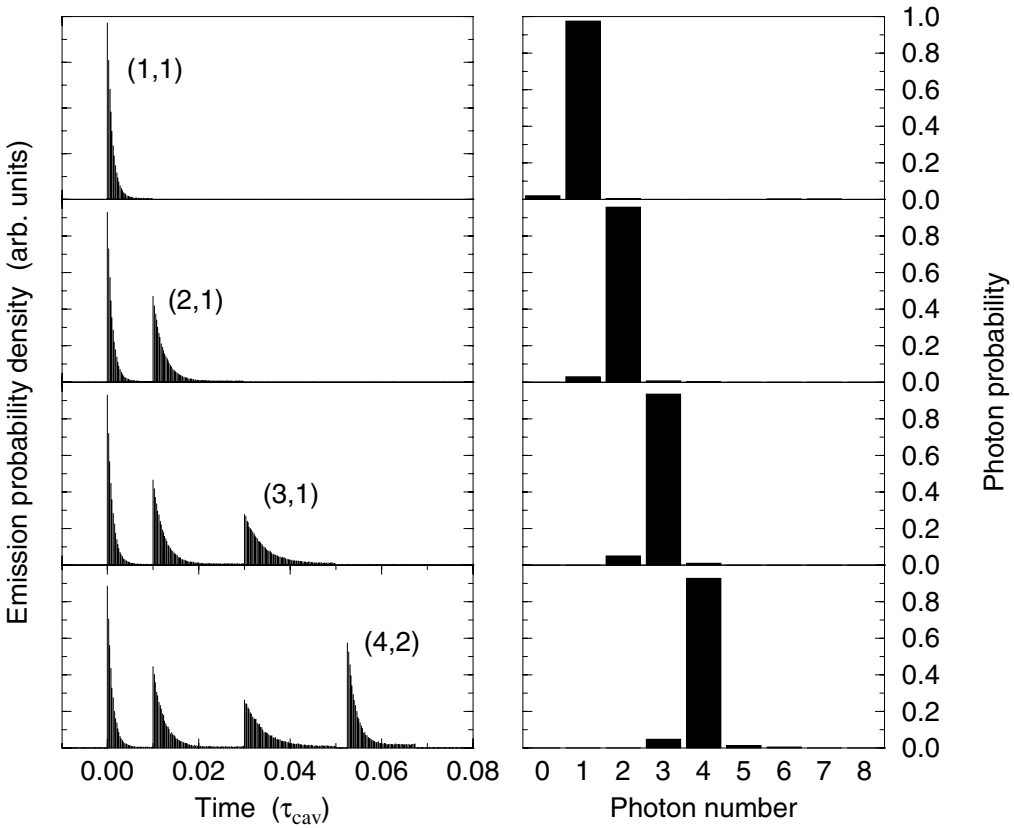

Figure 14. This figure shows one possible pulse sequence for creating Fock states of $n = 1$ to $n = 4$ in the cavity with a probability greater than 92% and based on no conditional measurements or stochastic probabilities. (a) The pulse sequences used and the probability distribution of lower state atoms within the pulses as a function of time from the start of the pulse sequence. (b) The cavity photon number remaining after the pulse sequence has been completed. The cavity is left in the target Fock state with a high probability. Pulse lengths used in this simulation were $|1\rangle = 2$ ms, $|2\rangle = 4$ ms, $|3\rangle = 4$ ms and $|4\rangle = 3$ ms. The conditions for the simulation were $\tau_{cav} = 200$ ms, $n_{th} = 10^{-4}$, $N_{ex} = 1500$ and $N_a = 15$, 30, 30 and 22.5, respectively.

hand, clearly relies on the controlled supply of single quantum states *on demand* [24]. From a more fundamental point of view, the quantum state reconstruction [29] of non-classical states requires the ability to create the same state repeatedly and reliably. Now that a robust method for creating Fock states is available, reconstruction of these highly non-classical states can be considered not just for the single-photon case but also for higher photon numbers.

References

[1] Meschede D *et al* 1985 *Phys. Rev. Lett.* **54** 551
[2] Scully M O and Zubairy M S 1997 *Quantum Optics* (Cambridge: Cambridge University Press)
[3] Jaynes E T and Cummings F W 1963 *Proc. IEEE* **51** 89

[4] Rempe G, Schmidt-Kaler F and Walther H 1990 *Phys. Rev. Lett.* **64** 2783
[5] Rempe G, Walther H and Klein N 1987 *Phys. Rev. Lett.* **58** 353
[6] Raithel G, Benson O and Walther H 1995 *Phys. Rev. Lett.* **75** 3446
[7] Benson O, Raithel G and Walther H 1994 *Phys. Rev. Lett.* **72** 3506
[8] Englert B-G, Löffler M, Benson O, Varcoe B, Weidinger M and Walther H 1998 *Fortschr. Phys.* **46** 897
[9] Leibfried D, Meekhof D M, King B E, Monroe C, Itano W M and Wineland D J 1996 *Phys. Rev. Lett.* **77** 4281
[10] Weidinger M, Varcoe B T H, Heerlein R and Walther H 1999 *Phys. Rev. Lett.* **82** 3795
[11] Varcoe B T H, Brattke S and Walther H 2000 *J. Opt. B: Quantum Semiclass. Opt.* **2** 154
[12] Brattke S, Varcoe B T H and Walther H 2001 *Opt. Express* **8** 131
[13] Varcoe B T H, Brattke S, Weidinger M and Walther H 2000 *Nature* **403** 743
[14] Brattke S, Englert B-G, Varcoe B T H and Walther H 2000 *J. Mod. Opt.* **47** 2857
[15] Brattke S, Varcoe B T H and Walther H 2001 *Phys. Rev. Lett.* **86** 3534
[16] Brattke S 2001 *PhD Thesis* University of Munich
[17] Nogues G, Rauschenbeutel A, Osnaghi S, Brune M, Raimond J M and Haroche S 1999 *Nature* **400** 239
[18] Brecha R J, Raithel G, Wagner C and Walther H 1993 *Opt. Commun.* **102** 257
[19] Raithel G, Wagner C, Walther H, Narducci L M and Scully M O 1994 *Advances in Atomic, Molecular and Optical Physics* Suppl. 2, ed P Berman (New York: Academic)
[20] Wiseman H and Milburn G 1993 *Phys. Rev. Lett.* **70** 548
[21] Krause J, Scully M O and Walther H 1987 *Phys. Rev.* A **36** 4547
[22] Bardoff P J, Mayr E and Schleich W P 1995 *Phys. Rev.* A **51** 4963
[23] Imamoglu A, Awschalom D D, Burkard G, DiVincenzo D P, Loss D, Sherwin M and Small A 1999 *Phys. Rev. Lett.* **83** 4204
Sherwin M, Imamoglu A and Montroy T 1999 *Phys. Rev.* A **60** 3508
An K, Childs J J, Dasari R R and Feld M S 1994 *Phys. Rev. Lett.* **73** 3375
[24] Gottesman D and Chuang L L 1999 *Nature* **402** 390
[25] Preskill J 1999 *Nature* **402** 357
Johnathon D and Plenio M B 1999 *Phys. Rev. Lett.* **83** 3566
[26] Vitali D, Tombesi P and Milburn G 1998 *Phys. Rev.* A **57** 4930
[27] Davidovich L, Zagury N, Brune M, Raimond J M and Haroche S 1994 *Phys. Rev.* A **50** R895
Cirac J I and Parkins A S 1994 *Phys. Rev.* A **50** R4441
Moussa M H Y 1997 *Phys. Rev.* A **55** R3287
[28] Briegel H-J, Englert B-G, Sterpi N and Walther H 1994 *Phys. Rev.* A **49** 2962
[29] Bodendorf C T, Antesberger G, Kim M S and Walther H 1998 *Phys. Rev.* A **57** 1371
Kim M S, Antesberger G, Bodendorf C T and Walther H 1999 *Phys. Rev.* A **58** R65 and references therein